Solid State Ionics 397 (2023) 116232

Contents lists available at ScienceDirect

Solid State Ionics

journal homepage: www.elsevier.com/locate/ssi

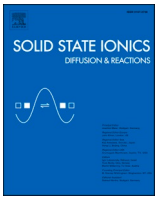

# Dynamical properties of the magnesium borohydride – ethylenediamine compound $Mg(en)_{1.2}(BH_4)_2$: A nuclear magnetic resonance study

O.A. Babanova [a,b], R.V. Skoryunov [a], A.V. Soloninin [a], I.E. Golub [c], M. Heere [d], A.V. Skripov [a,*], Y. Filinchuk [c]

[a] Institute of Metal Physics, Ural Branch of the Russian Academy of Sciences, Ekaterinburg 620108, Russia
[b] Ural Federal University, Ekaterinburg 620002, Russia
[c] Institute of Condensed Matter and Nanosciences, Université Catholique de Louvain, 1348 Louvain-la-Neuve, Belgium
[d] Institute of Internal Combustion Engines and Fuel Cells, Technische Universität Braunschweig, 38108 Braunschweig, Germany

ARTICLE INFO

*Keywords:*
Complex hydrides
Ionic conductors
Anion reorientations
Nuclear magnetic resonance

ABSTRACT

The magnesium borohydride – ethylenediamine (en) compound $Mg(en)_{1.2}(BH_4)_2$ exhibits high Mg-ion conductivity above room temperature. To study the dynamical properties of this compound and its partially deuterium-substituted counterpart, we have measured the $^1H$, $^2D$, and $^{11}B$ nuclear magnetic resonance (NMR) spectra and spin-lattice relaxation rates over a wide temperature range (6–324 K). Our measurements have revealed a coexistence of four types of $BH_4$ reorientational jump processes with different activation energies. For the fastest of these processes characterized by the activation energy of 47(3) meV, the unusually high reorientational mobility is retained down to low temperatures, so that the corresponding H jump rate is of the order of $10^8$ $s^{-1}$ near 70 K. The presence of fast reorientational motion of $[BH_4]^-$ anions in $Mg(en)_{1.2}(BH_4)_2$ supports the idea that anion reorientations may facilitate the cation diffusion. In the studied temperature range, we have not found any distinct signs of localized motion of the ethylenediamine molecules or their fragments at the NMR frequency scale.

## 1. Introduction

Magnesium borohydride $Mg(BH_4)_2$ is considered as a prospective hydrogen-storage material [1–5], due to its high hydrogen capacity (14.9 wt%). Furthermore, the stability of $Mg(BH_4)_2$ with respect to thermal decomposition appears to be lower than for other lightweight borohydrides: the pure $Mg(BH_4)_2$ starts to decompose at around 270 °C, that is, at a much lower temperature than Li and Na borohydrides [6]. The dehydrogenation properties of magnesium borohydride can be improved by additives, such as activated carbon [7], $TiCl_3$ [8], $TiF_3$ and $ScCl_3$ [9], or $Ni_3B$ and $Nb_2O_5$ [10]. In particular, it has been shown that the dehydrogenation – hydrogenation reaction in $Mg(BH_4)_2$ is partially reversible, and that the addition of 5 mol% of $TiF_3$ and $ScCl_3$ to $Mg(BH_4)_2$ significantly accelerates hydrogen desorption [9]. Another possible approach to improving dehydrogenation properties is based on using dihydrogen bonding ($H^{\delta-}\cdots H^{\delta+}$) [11,12] formed by the oppositely charged hydrogens ($H^{\delta-}$ and $H^{\delta+}$); this can be done by combining the $N–H^{\delta+}$ and $B–H^{\delta-}$ bonds in the same compound [13–15]. Recently, it has been found that ball milling $Mg(BH_4)_2$ with ethylenediamine (en) $NH_2CH_2CH_2NH_2$ in the molar ratios 1:2, 1:3, and 1:4 leads to the formation of $Mg(BH_4)_2$ – (en) composites with favorable dehydrogenation properties [16].

Apart from hydrogen-storage properties, some borohydride-based materials have attracted much recent attention as ionic conductors [17–23]. These materials represent a promising class of solid-state electrolytes for rechargeable batteries [24–28]. Since magnesium metal is an attractive anode material for such batteries due to its high volumetric capacity (3832 mAh/$cm^3$) and the Earth crust abundance of about 2% [29], it would be desirable to find solid-state electrolytes with sufficiently high Mg-ion conductivity [30]. However, the ionic conductivity of solid $Mg(BH_4)_2$ appears to be very poor ($< 10^{-12}$ S/cm at 30 °C), which has been attributed to the specific features of its structure [31]. Again, by combining the N–H and B–H bonds in the same compound, it was possible to increase the ionic conductivity, as demonstrated for $Mg(BH_4)(NH_2)$ [32], where $Mg^{2+}$ ions are tetrahedrally coordinated by two $[BH_4]^-$ and two $[NH_2]^-$ anions. Furthermore, the borohydride – ethylenediamine compound $Mg(en)_1(BH_4)_2$ has been reported to exhibit the ionic conductivity of $6 \times 10^{-5}$ S/cm at 70 °C [33].

* Corresponding author.
*E-mail address:* skripov@imp.uran.ru (A.V. Skripov).

https://doi.org/10.1016/j.ssi.2023.116232
Received 6 December 2022; Received in revised form 30 March 2023; Accepted 11 April 2023
Available online 28 April 2023

Recent structural study [34] has shown that the true composition of this conducting phase is $Mg(en)_{1.2}(BH_4)_2$, i.e. it exhibits the 5:6 stoichiometric Mg to (en) ratio. The complex structure of $Mg(en)_{1.2}(BH_4)_2$ was solved in the triclinic space group $P-1$ using single-crystal synchrotron X-ray diffraction and confirmed by neutron powder diffraction [34].

The important dynamical feature of borohydrides is that $[BH_4]^-$ anions can participate in the fast reorientational (rotational) motion [35,36]. This motion strongly contributes to the balance of energies determining thermodynamic stability; therefore, information on the anion reorientations is crucial for understanding the fundamental properties of borohydrides. It has been shown that reorientational dynamics of the anions in borohydrides depends on the coordination environment of $BH_4$ groups [37,38]; in certain cases, the anion dynamics can be described in terms of the low-temperature rotational tunneling [38]. Furthermore, the reorientational (rotational) motion of $[BH_4]^-$ anions may play a significant role in the mechanisms of ionic conductivity in borohydride-based systems [39–44], facilitating fast cation diffusion. In the present work, we report the results of detailed investigation of dynamical properties of the magnesium borohydride – ethylenediamine compound $Mg(en)_{1.2}(BH_4)_2$ and its partially deuterium-substituted counterpart using $^1H$, $^2D$, and $^{11}B$ nuclear magnetic resonance (NMR) measurements of the spectra and spin-lattice relaxation rates over a wide temperature range (6–324 K). The parameters of H jump motion derived from our NMR data for $Mg(en)_{1.2}(BH_4)_2$ are discussed in connection with the structural features of this compound.

## 2. Experimental details

All sample manipulations were performed in glove-boxes filled with dry argon ($\geq$ 99.999%) and with oxygen and water levels not exceeding 1 ppm. All commercial compounds were used as received without any purification. The synthesis of $Mg(en)_{1.2}(BH_4)_2$ complex was analogous to that described in Ref. [34]. At the first stage, magnesium borohydride, γ-$Mg(BH_4)_2$, was prepared following the synthetic procedure described in Ref. [45]. Next, $Mg(en)_3(BH_4)_2$ was obtained by ball milling γ-$Mg(BH_4)_2$ with ethylenediamine (99%, Acros Organics) with a Fritsch Pulverisette 7 premium line apparatus using 10:1 ball-to-powder mass ratio at 300 rpm for 3 periods of 10 min milling time, interrupted by 5 min of cooling breaks. The excess of (en) was subsequently removed under dynamic vacuum at 120 °C for 1 h. At the final stage, $Mg(en)_{1.2}(BH_4)_2$ was prepared by ball milling [46] a mixture of $Mg(en)_3(BH_4)_2$ and γ-$Mg(BH_4)_2$ (2:3 M ratio, 60:1 ball-to-powder mass ratio, 9 periods of 2 min milling time, interrupted by 5 min of cooling breaks) followed by annealing at 70 °C for 3 h in a reactor made of Swagelok stainless steel parts placed in tubular oven or on a Schlenk line, under dynamic vacuum of an oil pump. More details of the synthesis and characterization are reported in Ref. [34]. On the basis of single-crystal synchrotron X-ray diffraction analysis, the structure of $Mg(en)_{1.2}(BH_4)_2$ is solved to be triclinic (space group $P-1$) with the lattice parameters $a = 7.1569(10)$ Å, $b = 12.1915(23)$ Å, $c = 12.5351(17)$ Å, $\alpha = 99.43(1)°$, $\beta = 103.99(1)°$, $\gamma = 90.46(1)°$ [34]. This structure contains four crystallographically inequivalent ethylenediamine molecules and five $BH_4^-$ groups. The schematic view of this structure is shown in Fig. 1. The partially deuterated sample $Mg(en)_{1.2}(BD_4)_2$ was prepared in the same way, however, the deuterium-substituted γ-$Mg(BD_4)_2$ was used as a starting compound; for ethylenediamine, there were no isotope substitution. The neutron powder diffraction analysis performed on the deuterated sample [34] has confirmed the structure of Mg borohydride – ethylenedimine compound (Fig. S1 of the Supplementary Information). Included in the Supplementary Information are also the synchrotron X-ray powder diffraction pattern (Fig. S2), Table S1 with the structural parameters, and the $^{11}B$ magic-angle-spinning NMR spectra (Fig. S3) [34].

For NMR experiments, the samples were flame-sealed in quartz tubes under vacuum. Low-field $^1H$ and $^{11}B$ NMR measurements of the spectra and spin-lattice relaxation rates were performed on a pulse spectrometer

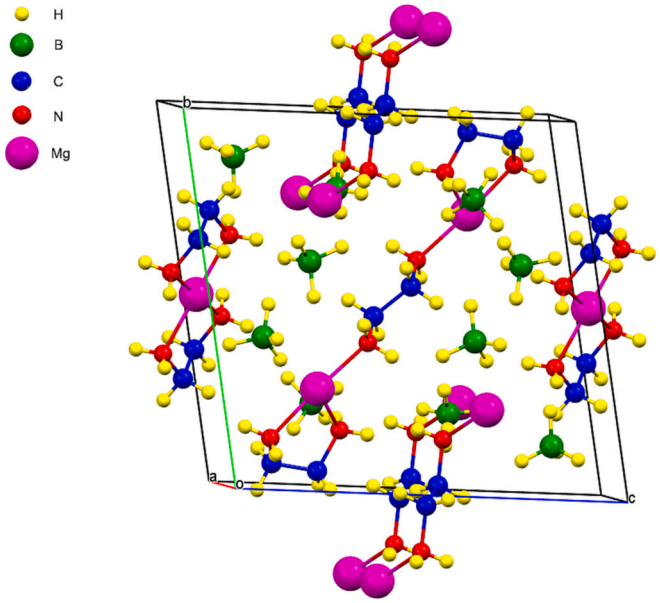


**Fig. 1.** Schematic view of the unit cell of $Mg(en)_{1.2}(BH_4)_2$.

with quadrature phase detection at the frequencies $\omega/2\pi = 14$ MHz ($^1H$) and 28 MHz ($^1H$ and $^{11}B$). The magnetic field was provided by a 2.1 T iron-core Bruker magnet. A home-built multinuclear continuous-wave NMR magnetometer working in the range 0.32–2.15 T was used for field stabilization. For rf pulse generation, we used a home-built computer-controlled pulse programmer, the PTS frequency synthesizer (Programmed Test Sources, Inc.), and a 1 kW Kalmus wideband pulse amplifier. Typical values of the $\pi/2$ pulse length were 2–3 μs for both $^1H$ and $^{11}B$. NMR cell with the sample was placed into an Oxford Instruments CF1200 continuous-flow cryostat using helium or nitrogen as a cooling agent. The sample temperature, monitored by a chromel-(Au—Fe) thermocouple, was stable to ±0.1 K. High-field $^2D$ NMR measurements were performed on a Bruker AVANCE III 500 spectrometer at the frequency $\omega/2\pi = 76.7$ MHz. The $\pi/2$ pulse length for the $^2D$ NMR measurements was 6 μs. The nuclear spin-lattice relaxation rates were measured using the saturation–recovery method. In all cases, the recovery of nuclear magnetization could be reasonably approximated by a single exponential function. NMR spectra were recorded by Fourier transforming the solid echo signals (pulse sequence $\pi/2_x - t - \pi/2_y$).

## 3. Results and discussion

### 3.1. Overview of the $^1H$, $^2D$ and $^{11}B$ NMR results

Temperature dependences of the proton spin-lattice relaxation rates $R_1^H$ for $Mg(en)_{1.2}(BH_4)_2$ measured at two resonance frequencies $\omega/2\pi$ (14 and 28 MHz) are shown in Fig. 2. As it can be seen from the figure, $R_1^H(T)$ exhibits two frequency-dependent maxima at the temperatures near 90 K and 220 K. Such maxima are typical of the spin-lattice relaxation mechanism due to motionally-modulated dipole-dipole interactions between nuclear spins [47]; they are expected to occur at the temperatures at which the corresponding H jump rate $\tau^{-1}$ becomes nearly equal to the (circular) resonance frequency $\omega$. In our case, $\omega$ is of the order of $10^8$ $s^{-1}$. Thus, the position of the $R_1^H(T)$ peak may serve as an indicator of the H mobility in different systems. For the systems with higher H jump rates, the $R_1^H(T)$ peak is expected to occur at lower temperatures.

It should be noted that the positions of the $R_1^H(T)$ peaks for $Mg(en)_{1.2}(BH_4)_2$ differ considerably from the corresponding positions for all the crystalline $Mg(BH_4)_2$ phases studied so far [37,48–50]. Indeed, for the crystalline α, β, and γ phases of $Mg(BH_4)_2$, the $R_1^H(T)$ maxima at

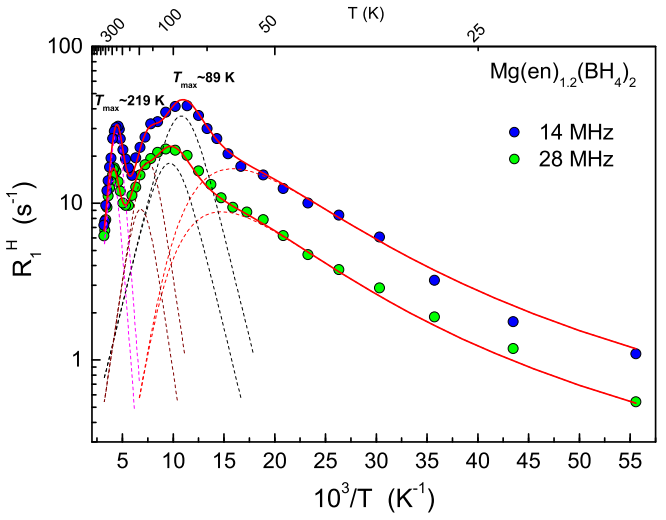


**Fig. 2.** Proton spin-lattice relaxation rates measured at 14 and 28 MHz for Mg(en)$_{1.2}$(BH$_4$)$_2$ as functions of the inverse temperature. The temperatures of the relaxation rate maxima at 14 MHz are shown near the corresponding peaks. The red solid curves show the simultaneous fit of the four-peak model to the data over the temperature range of 18–315 K. The dashed curves show individual contributions of the four peaks to the fit. (For interpretation of the references to colour in this figure legend, the reader is referred to the web version of this article.)

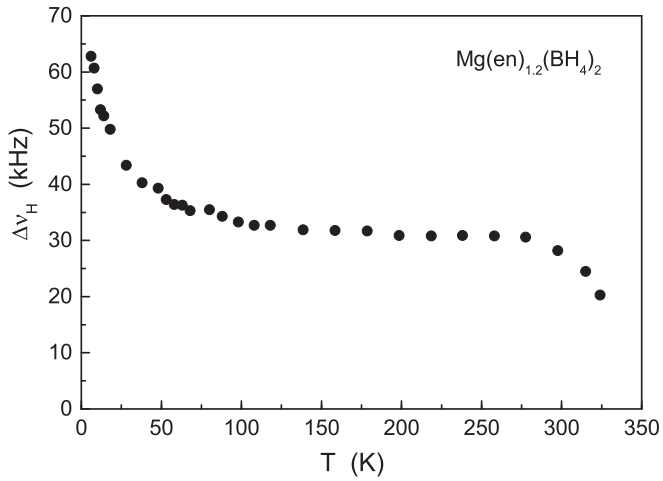


**Fig. 3.** Temperature dependence of the width (full width at half-maximum) of the $^1$H NMR spectrum for Mg(en)$_{1.2}$(BH$_4$)$_2$ at 28 MHz.

$\omega/2\pi = 14$ MHz are observed near 290 K [48], 120 K [37], and 270 K [37], respectively. This means that Mg(en)$_{1.2}$(BH$_4$)$_2$ exhibits its own distinct H dynamics. Furthermore, for the amorphous Mg(BH$_4$)$_2$ phase, the $R_1^H(T)$ maximum at $\omega/2\pi = 14$ MHz occurs near 190 K [51]; the absence of such a peak for Mg(en)$_{1.2}$(BH$_4$)$_2$ suggests that our sample does not contain any significant fraction of the amorphous Mg(BH$_4$)$_2$ phase (which could have appeared in the course of synthesis [34]). The observation of the main $R_1^H(T)$ maximum near 90 K in Mg(en)$_{1.2}$(BH$_4$)$_2$ (Fig. 2) indicates that a considerable fraction of H atoms in this compound participate in the very fast jump motion even at low temperatures. It should be noted that even below 70 K the measured proton relaxation rates remain to be quite high showing the well-defined frequency dependence; these features suggest that the relaxation behavior in this region is still dominated by the reorientational motion of H atoms.

The existence of fast H jump motion down to low temperatures is also supported by the behavior of the width of $^1$H NMR spectrum. The evolution of the proton NMR spectra with temperature is shown in Fig. S4 of the Supplementary Information, and the temperature dependence of the full width at half-maximum of this spectrum, $\Delta\nu_H$, is presented in Fig. 3. Usually, the low-temperature width of the proton NMR spectrum, $\Delta\nu_{HR}$, is determined by static ('rigid lattice') dipole-dipole interactions of $^1$H spins, and the step-like line narrowing is observed when the jump rate $\tau^{-1}$ exceeds $\Delta\nu_{HR}$ [47]. For complex hydrides, the values of $\Delta\nu_{HR}$ are typically of the order of $10^5$ s$^{-1}$ [40]. As can be seen from Fig. 3, the onset of the motional narrowing of the proton NMR spectrum occurs at very low temperatures (~ 15 K or below). Furthermore, even at 6 K, the $^1$H NMR line width is smaller than that expected for the "rigid lattice". Indeed, calculations of the second moment for the "rigid lattice" dipole-dipole interactions of $^1$H spins based on the structure of Mg(en)$_{1.2}$(BH$_4$)$_2$ [34] give the value of $4.28 \times 10^{10}$ s$^{-2}$. For a Gaussian shape of the spectrum, this corresponds to the line width of 77.7 kHz; the observed value of $\Delta\nu_H$ at 6 K (62.2 kHz) appears to be considerably smaller. While this comparison may suggest that the H jump motion is not completely "frozen" at the NMR frequency scale, it should be noted that the shape of the low-$T$ proton NMR line is not Gaussian (see Fig. S4 of the Supplementary Information). For some complex borohydrides, the absence of H "freezing out" at low temperatures may originate from the rotational tunneling [52] of BH$_4$ groups, as revealed in the lithium benzimidazolate-borohydride Li$_2$(bIm)BH$_4$ by combining NMR, quasielastic neutron scattering and neutron spin-echo measurements [38]. However, the rotational tunneling is expected to lead to the proton spin-lattice relaxation rate maximum in the range of 20–30 K [38], i.e., at much lower temperatures than in the case of Mg(en)$_{1.2}$(BH$_4$)$_2$.

The value of $\Delta\nu_H$ remains nearly constant over the temperature range of 100–280 K. Such a high-temperature plateau regime is typical of borohydrides and the related compounds [42], where the reorientational (localized) motion cannot fully average out the dipole-dipole interactions of $^1$H spins, even in the limit of $\Delta\nu_{HR}\tau << 1$. However, above 300 K, the line width starts to decrease again (see Fig. 3). This behavior suggests the excitation of an additional motional process at the NMR frequency scale. The nature of this process remains unknown, since we have not performed any measurements above 324 K; such an upper limit was set in order to avoid a possible formation of other phases at higher temperatures [34].

The presence of two $R_1^H(T)$ maxima in Mg(en)$_{1.2}$(BH$_4$)$_2$ (Fig. 2) indicates that there are at least two types of H jump motion with different parameters. In borohydride-based compounds, the observed $R_1^H(T)$ peaks are usually associated with different types of reorientations of [BH$_4$]$^-$ anions [40,42]. In Mg(en)$_{1.2}$(BH$_4$)$_2$, both the [BH$_4$]$^-$ anions and the (en) ligands contain H atoms; therefore, additional experiments are necessary for the peak assignment. One of such experiments is the $^1$H spin-lattice relaxation rate measurement for the sample with deuterium substitution in the anions, Mg(en)$_{1.2}$(BD$_4$)$_2$. In Fig. 4, the results of the $^1$H relaxation rate measurements for Mg(en)$_{1.2}$(BD$_4$)$_2$ at $\omega/2\pi = 28$ MHz are compared with those for Mg(en)$_{1.2}$(BH$_4$)$_2$ in the temperature range of 73–315 K. It can be seen that both the low-temperature and the high-temperature $R_1^H(T)$ peaks for Mg(en)$_{1.2}$(BH$_4$)$_2$ disappear for the deuterium-substituted Mg(en)$_{1.2}$(BD$_4$)$_2$. This means that both $R_1^H(T)$ peaks for Mg(en)$_{1.2}$(BH$_4$)$_2$ should be attributed to reorientations of the [BH$_4$]$^-$ anions. Although the measured $^1$H relaxation rate in Mg(en)$_{1.2}$(BD$_4$)$_2$ is not strictly temperature-independent, it changes by less than a factor of 2 over the very wide temperature range of 80–298 K. Such a behavior can hardly be ascribed to any thermally activated atomic motion.

Another experiment supporting this assignment of the peaks is represented by the $^{11}$B spin-lattice relaxation measurements. Since B atoms are close to H atoms of the [BH$_4$]$^-$ anions, being rather far away from H atoms of the ethylenediamine ligands, it may be expected that the measured $^{11}$B spin-lattice relaxation rates, $R_1^B$, are sensitive to anion reorientations, but not sensitive to H jumps in the (en) groups. The results of the $R_1^B$ measurements for Mg(en)$_{1.2}$(BH$_4$)$_2$ at 28 MHz are shown

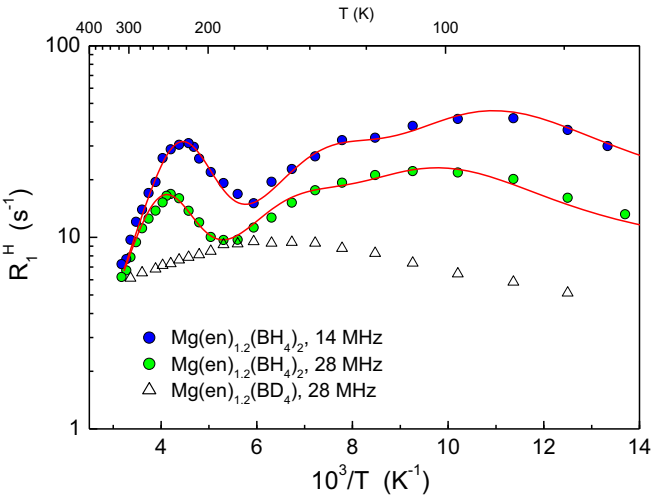


**Fig. 4.** Comparison of the proton spin-lattice relaxation rates for Mg(en)$_{1.2}$(BH$_4$)$_2$ and Mg(en)$_{1.2}$(BD$_4$)$_2$ as functions of the inverse temperature. The red solid curves show the simultaneous fit of the four-peak model to the data for Mg(en)$_{1.2}$(BH$_4$)$_2$. For this compound, the data and the fits are the same as those in Fig. 2, although in the limited temperature range. (For interpretation of the references to colour in this figure legend, the reader is referred to the web version of this article.)

in Fig. 5. As can be seen from this figure, the behavior of $R_1^B(T)$ is similar to that for $R_1^H(T)$; it shows two peaks at the temperatures close to the temperatures of the corresponding $^1$H relaxation rate peaks. This allows us to conclude that both the observed $^1$H and $^{11}$B spin-lattice relaxation rates are dominated by H jumps in the reorienting BH$_4$ groups. Comparison of the $^{11}$B relaxation rates in Mg(en)$_{1.2}$(BH$_4$)$_2$ and Mg(en)$_{1.2}$(BD$_4$)$_2$ (see Fig. S5 of the Supplementary Information) is consistent with the absence of strong isotope effects for the reorientational jump rates of BH$_4$ (BD$_4$) tetrahedra.

The evolution of $^2$D NMR spectra for Mg(en)$_{1.2}$(BD$_4$)$_2$ is presented in Fig. S6 of the Supplementary Information, and the behavior of the $^2$D spin-lattice relaxation rate $R_1^D$ for this compound is shown in Fig. 6. In contrast to $^1$H, deuterium nuclei with the spin $I_D = 1$ have non-zero electric quadrupole moments; therefore, the effects related to quadrupole splitting in the $^2$D NMR spectra (Fig. S6) can be expected. In particular, the $^2$D NMR spectra above 160 K show distinct signs of a quadrupole line with the splitting of about 24 kHz that coexists with a

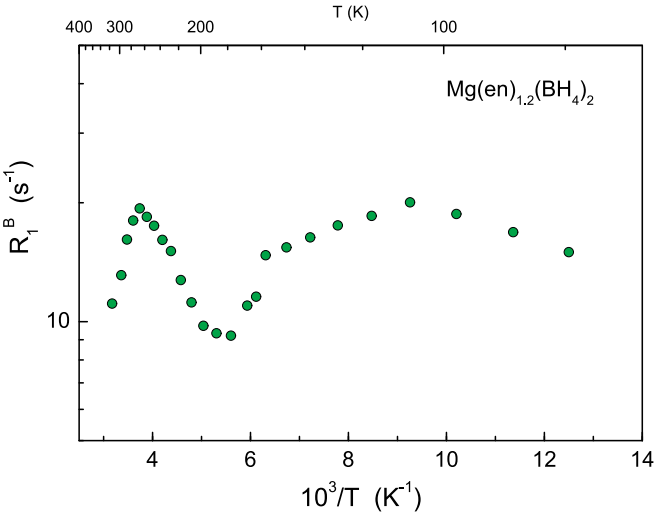


**Fig. 5.** $^{11}$B spin-lattice relaxation rate measured at 28 MHz for Mg(en)$_{1.2}$(BH$_4$)$_2$ as a function of the inverse temperature.

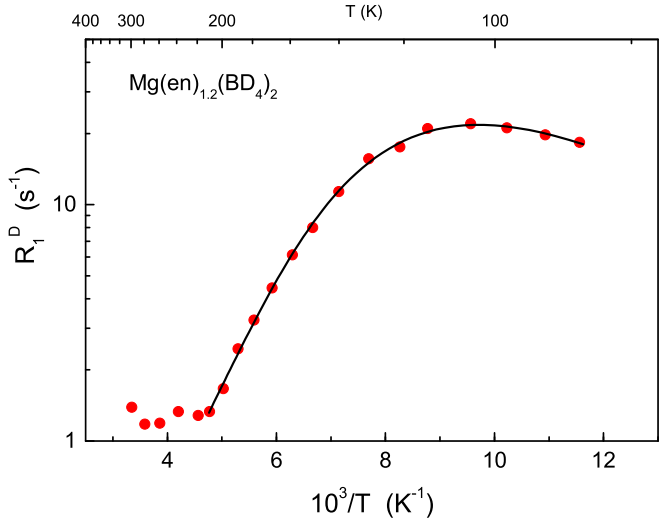


**Fig. 6.** $^2$D spin-lattice relaxation rate measured at 76 MHz for Mg(en)$_{1.2}$(BD$_4$)$_2$ as a function of the inverse temperature. The solid curve shows a fit of the model with a Gaussian distribution of the activation energies to the data in the range of 86–210 K.

narrow central line. However, at lower temperatures, the split line seems to disappear. It should be noted that due to technical limitations, our $^2$D NMR measurements were performed only down to 83 K, where the reorientational motion remains to be quite fast at the NMR frequency scale. This means that even at 83 K, the $^2$D quadrupole interaction may be averaged. The behavior of $R_1^D(T)$ for Mg(en)$_{1.2}$(BD$_4$)$_2$ appears to be quite remarkable. As can be seen from Fig. 6, the $^2$D spin-lattice relaxation rate exhibits the pronounced peak near 100 K, i.e. in the range of the low-temperature $R_1^H(T)$ peak for Mg(en)$_{1.2}$(BH$_4$)$_2$ (see Fig. 2). However, in the range of the high-temperature $R_1^H(T)$ peak for Mg(en)$_{1.2}$(BH$_4$)$_2$, we do not observe any $R_1^D(T)$ peak for Mg(en)$_{1.2}$(BD$_4$)$_2$.

In order to interpret these results, we have to consider possible mechanisms of the $^2$D spin-lattice relaxation. If the relaxation is determined by fluctuations of dipole-dipole interactions, the corresponding relaxation rate should be proportional to the square of the nuclear gyromagnetic ratio $\gamma$. Furthermore, the maximum relaxation rate should be inversely proportional to the resonance frequency $\omega$ [47]. Thus, for the same type of motion, the expected ratio of the maximum $^1$H and $^2$D relaxation rates is $\gamma_H^2\omega_D/\gamma_D^2\omega_H$. Since $\gamma_H/\gamma_D = 6.51$, for $\omega_D/2\pi = 76$ MHz and $\omega_H/2\pi = 14$ MHz, we obtain the expected maximum relaxation rate ratio of 230. For the low-temperature peak, the expected maximum $^2$D relaxation rate is 0.18 $s^{-1}$, while the observed one is 21.7 $s^{-1}$. The fact that the observed maximum $^2$D relaxation rate is much higher than the one expected for fluctuating dipole-dipole interactions indicates that the low-temperature relaxation rate peak in Mg(en)$_{1.2}$(BD$_4$)$_2$ is dominated by fluctuating quadrupole interactions. On the other hand, we may assume that the absence of any observable $R_1^D(T)$ peak at higher temperatures is related to its small amplitude, in accordance with our estimates for the dipole-dipole interaction. If, in addition to the very small dipole-dipole contribution, the high-temperature motional process does not lead to strong electric-field-gradient (EFG) fluctuations at D sites (which seems probable, since the quadrupole splitting is not averaged out at these temperatures), then some background relaxation mechanisms may start to govern the measured $^2$D relaxation rate.

### 3.2. Model description of the $^1$H and $^2$D spin-lattice relaxation data

For parametrization of the proton spin-lattice relaxation data for Mg(en)$_{1.2}$(BH$_4$)$_2$, we have used the approach analogous to that employed for α-Mg(BH$_4$)$_2$ [48]. It is based on a coexistence of several reorientational processes with the jump rates $\tau_i^{-1}$; for each of the processes, the

temperature dependence of the jump rate is expected to follow an Arrhenius law with the activation energy $E_{ai}$,

$$\tau_i^{-1} = \tau_{0i}^{-1} exp(-E_{ai}/k_B T), \quad (1)$$

where $k_B$ is the Boltzmann constant. The observed proton spin-lattice relaxation rate in this model is expressed as the sum of contributions $R_{1i}^H$ from each of the reorientational processes, where $R_{1i}^H$ is determined by combining the standard expression that relates the spin-lattice relaxation rate with $\tau_i^{-1}$ (see Supplementary Information) and the Arrhenius law (Eq. (1)) for the $i$th process. According to the theory of nuclear spin-lattice relaxation due to atomic motion [47], each reorientational process is expected to give rise to the $R_{1i}^H(T)$ peak at $\omega\tau_i \approx 1$, while in the limit of slow motion ($\omega\tau_i >> 1$), $R_{1i}^H$ should be proportional to $\omega^{-2}\tau_i^{-1}$, and in the limit of fast motion ($\omega\tau_i << 1$), $R_{1i}^H$ should be proportional to $\tau_i$, being frequency-independent. Inspection of the data in Fig. 2 shows that two overlapping peaks are not sufficient for description of the experimental results with a number of inflection points. We have found that the appropriate model should include four relaxation rate peaks, which means a coexistence of four reorientational processes with different parameters. Possible reasons for such a coexistence will be discussed below. The model parameters are the activation energies $E_{ai}$, the pre-exponential factors of the Arrhenius law, $\tau_{0i}$, and the amplitude factors $\Delta M_i$ characterizing the strength of fluctuating dipole-dipole interactions for each of the processes ($i = 1, 2, 3, 4$). We assume that the fastest process corresponds to $i = 1$, and the slowest one corresponds to $i = 4$. It should be noted that, for the fastest reorientational process, the frequency dependence of the relaxation rate at $T < 40$ K appears to be considerably weaker than the predicted $\omega^{-2}$ dependence for the slow-motion limit. This feature suggests a presence of a certain distribution of jump rates [53] for the fastest process; therefore, the dispersion $\Delta E_{a1}$ of the activation energy distribution for this process has been introduced as the additional model parameter (see Supplementary Information for details). Using the same approach as that in Ref. [48], we look for a set of parameters giving the best fit to the $R_{1i}^H(T)$ data at two resonance frequencies *simultaneously*. The results of such a simultaneous fit are shown by red solid curves in Fig. 2; the dashed curves in this figure correspond to individual contributions of the four peaks. The parameters resulting from the fit are included in Table 1.

It should be noted that the value of $E_{a4}$ is in the range of activation energies for $[BH_4]^-$ reorientations in regular borohydrides [36]. On the other hand, the small values of $E_{a1}$, $E_{a2}$, and $E_{a3}$ are typical of those borohydride-based systems that retain very high reorientational mobility down to low temperatures [40,42].

In order to discuss possible reasons for a coexistence of several reorientational jump processes, we have to consider the local coordination of $BH_4$ groups. According to the structural studies [34], there are 5 crystallographically inequivalent $BH_4$ groups in $Mg(en)_{1.2}(BH_4)_2$; the local coordination of these groups is schematically presented in Fig. 7. As can be seen from this figure, the local environment changes significantly from one $BH_4$ group to another. For configuration *a*), the tetrahedral $BH_4$ group is nearly linearly coordinated by two $Mg^{2+}$ ions via the edges. For configurations *b*), *c*), and *d*), the $BH_4$ group is coordinated by a single $Mg^{2+}$ ion via the tetrahedron edge, and for configuration *e*), this group is coordinated by a single $Mg^{2+}$ ion via the tetrahedron face. It should be noted that, even for a single crystallographically independent $BH_4$ group, we may expect a coexistence of several reorientational processes with different motional parameters due to the possibility of rotations around different symmetry axes [42]. For example, the case of two coexisting reorientational processes for equivalent $BH_4$ groups is well-documented for the low-temperature (orthorhombic) phase of $LiBH_4$ [54,55]. In the case of several inequivalent $BH_4$ groups, there are more opportunities for coexisting reorientations, and a single-exponential spin-lattice relaxation may result from the rapid equalization of the $^1H$ spin polarization (*spin diffusion*) [56] due to strong $^1H - ^1H$ dipole-dipole interactions.

On the basis of the available data, we cannot assign the observed jump processes in $Mg(en)_{1.2}(BH_4)_2$ to particular types of reorientations. However, two types of environments are known to be favorable for the fast $BH_4$ reorientations in other borohydride-based systems. One of these environments is the nearly linear coordination of the $BH_4$ tetrahedron by two $Mg^{2+}$ ions via the edges (configuration *a*) in Fig. 7). In this case, the 2-fold symmetry axis along the Mg – B – Mg line is expected to be the "easy" reorientational axis corresponding to the lowest activation energy, since the rotation around this axis does not break any of the four Mg···H interactions [48]. The other favorable environment corresponds to the coordination of the $BH_4$ tetrahedron by a single $Mg^+$ ion via the triangular face (configuration *e*) in Fig. 7). In this case, the rotation around the 3-fold symmetry axis along the Mg – B line does not break any of the three Mg···H interactions. Thus, it is reasonable to attribute the fastest reorientational processes in $Mg(en)_{1.2}(BH_4)_2$ with the lowest activation energies to these two types of $BH_4$ reorientations.

For parametrization of the low-temperature $^2D$ spin-lattice relaxation data for $Mg(en)_{1.2}(BD_4)_2$, we have used the simplest approach describing the motionally-induced quadrupole contribution to the spin-lattice relaxation rate; this approach is based on the expression

$$R_1^D = \frac{M_Q}{\omega}\left[\frac{y}{1+y^2} + \frac{4y}{1+4y^2}\right], \quad (2)$$

where $y = \omega\tau$. Here the amplitude factor $M_Q$ is proportional to the square of the electric quadrupole moment of $^2D$ and the mean square of the fluctuating part of the electric field gradient (EFG) at $^2D$ sites due to the reorientational jumps. It should be noted that the basic features of the dependence of this quadrupole contribution on $\omega$ and $\tau$ are similar to those of the motionally-induced dipole-dipole contribution; however, the amplitude factor is different. We assume that the temperature dependence of $\tau$ is governed by the Arrhenius law. Furthermore, as in the case of the low-temperature $^1H$ relaxation results, the observed $^2D$ relaxation peak suggests the presence of a certain distribution of jump rates. Therefore, our model parameters include the average activation energy $E_a$, the dispersion $\Delta E_a$ of the activation energy distribution, the pre-exponential factor $\tau_0$, and the amplitude factor $M_Q$. These parameters have been varied to find the best fit of the model to the experimental $R_1^D(T)$ data in the range of 86–210 K. The resulting fit is shown by the solid curve in Fig. 6; the corresponding fit parameters: $E_a = 75(8)$ meV, $\Delta E_a = 19(7)$ meV, $\tau_0 = 1.6(4) \times 10^{-13}$ s, and $M_Q = 1.5(3) \times 10^{10}$ s$^{-2}$. It is interesting to note that the average value of $E_a$ derived from the low-temperature $^2D$ spin-lattice relaxation data lies between the activation energies $E_{a2}$ and $E_{a3}$ determining the behavior of the $^1H$ spin-lattice relaxation rate in the region of the low-temperature peak.

**Table 1**
Parameters resulting from the simultaneous fit of the $R_1^H(T)$ data to the four-peak model.

| $i$ | $E_a$ (meV) | $\Delta E_a$ (meV) | $\tau_0$ (s) | $\Delta M$ (s$^{-2}$) |
|---|---|---|---|---|
| 1 | 47(3) [a] | 18(1) | $6.1(4) \times 10^{-13}$ | $1.4(1) \times 10^9$ |
| 2 | 52(3) | – | $1.6(1) \times 10^{-11}$ | $1.0(1) \times 10^9$ |
| 3 | 86(4) | – | $6.2(1) \times 10^{-12}$ | $5.1(4) \times 10^8$ |
| 4 | 171(5) | – | $1.7(1) \times 10^{-12}$ | $7.9(5) \times 10^8$ |

[a] Average activation energy for a Gaussian distribution.

## 4. Conclusions

The results of our $^1H$ and $^{11}B$ NMR measurements indicate that $BH_4$ groups in the magnesium borohydride – ethylenediamine compound $Mg(en)_{1.2}(BH_4)_2$ retain unusually high reorientational mobility down to low temperatures. Indeed, a partial motional narrowing of the proton NMR spectra is observed even below 20 K. The analysis of the $^1H$ spin-lattice relaxation rates has revealed a coexistence of four types of $BH_4$ reorientational jump processes with different activation energies. The

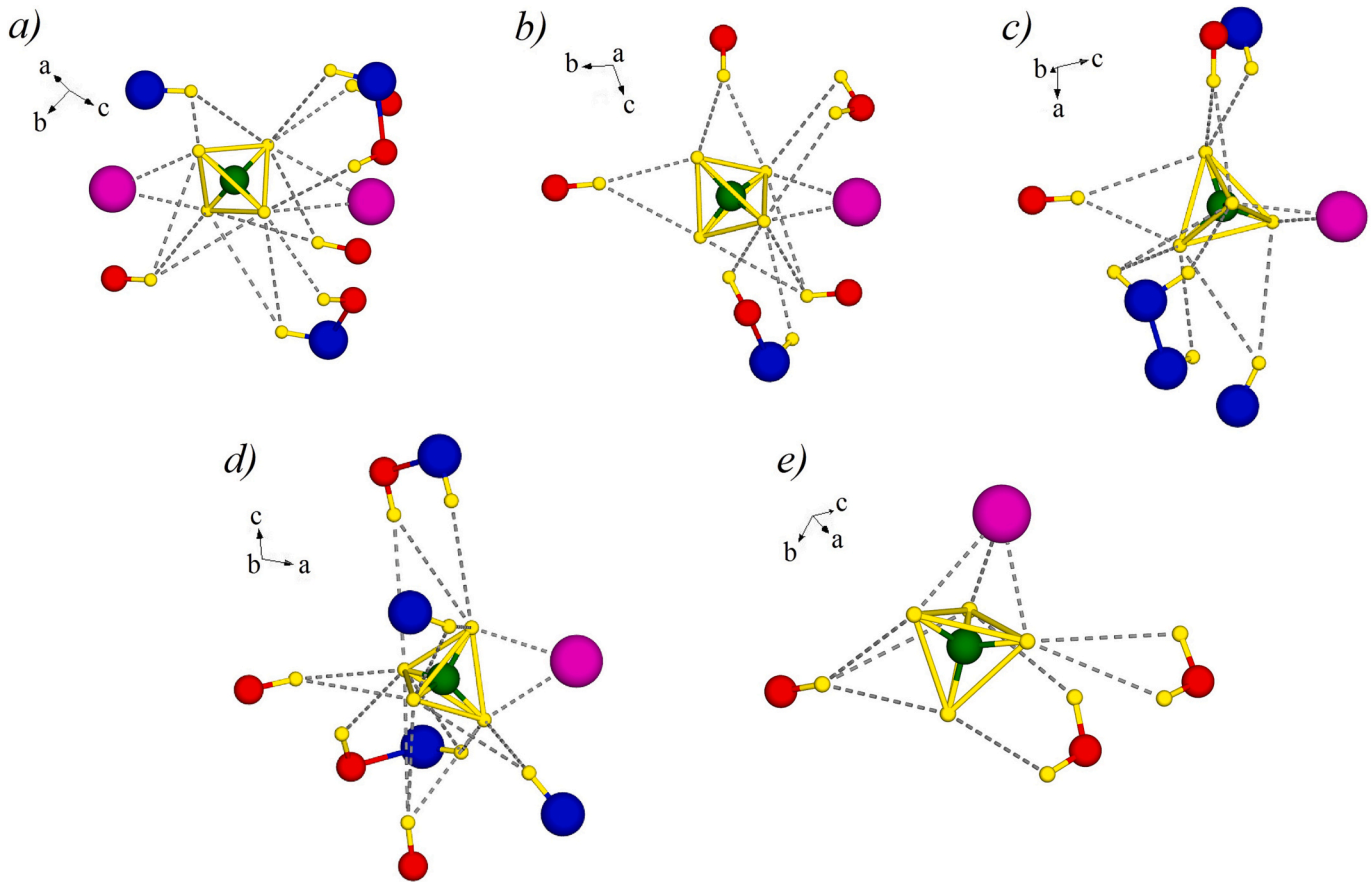


**Fig. 7.** Schematic view of the coordination environment of 5 inequivalent tetrahedral $BH_4$ groups in $Mg(en)_{1.2}(BH_4)_2$. Magenta spheres: Mg atoms, blue spheres: C atoms, red spheres: N atoms, green spheres: B atoms, and yellow spheres: H atoms. The dashed gray lines show the Mg···H and H···H bonds for H atoms in $BH_4$ groups. (For interpretation of the references to colour in this figure legend, the reader is referred to the web version of this article.)

fastest of these processes is characterized by the average activation energy of 47(3) meV, and the corresponding H jump rate reaches $\sim 10^8$ $s^{-1}$ already near 70 K. On the basis of the local coordination of crystallographically inequivalent $BH_4$ groups in $Mg(en)_{1.2}(BH_4)_2$, we suggest two possible types of reorientations with low energy barriers. It should be noted that the presence of fast $BH_4$ reorientations in the compound showing rather high Mg-ion conductivity supports the idea that anion reorientations may facilitate the cation diffusion. In the studied temperature range up to 320 K, we have not found any distinct signs of localized motion of the ethylenediamine molecules or their fragments at the NMR frequency scale. However, these molecules play an important role in stabilizing the unusual complex structure of $Mg(en)_{1.2}(BH_4)_2$.

## CRediT authorship contribution statement

**O.A. Babanova:** Investigation, Software, Formal analysis, Writing – original draft. **R.V. Skoryunov:** Investigation, Visualization. **A.V. Soloninin:** Investigation, Methodology, Validation. **I.E. Golub:** Investigation, Writing – review & editing. **M. Heere:** Writing – review & editing. **A.V. Skripov:** Supervision, Writing – review & editing. **Y. Filinchuk:** Methodology, Writing – review & editing.

## Declaration of Competing Interest

The authors declare that they have no known competing financial interests or personal relationships that could have appeared to influence the work reported in this paper.

## Data availability

Data will be made available on request.

## Acknowledgments

This work was performed within the assignment of the scientific program “Function” (No. 122021000035-6) of the Ural Branch of the Russian Academy of Sciences. We acknowledge Fédération Wallonie-Bruxelles (ARC 18/23-093 MicroBat) and Fonds National de la Recherche Scientifique (T.0169-13, U.N036.15, U·N022-19, J.0073-20) for funding.

## Appendix A. Supplementary data

The results of the structural characterization, room-temperature $^{11}B$ MAS-NMR spectra, evolution of the measured $^{1}H$ and $^{2}D$ NMR spectra with temperature, comparison of the measured $^{11}B$ spin-lattice relaxation rates in $Mg(en)_{1.2}(BH_4)_2$ and $Mg(en)_{1.2}(BD_4)_2$, as well as expressions used for analysis of the proton spin-lattice relaxation rates. These materials can be found online at.

## References

[1] S. Orimo, Y. Nakamori, J.R. Elisen, A. Züttel, C.M. Jensen, Complex hydrides for hydrogen storage, Chem. Rev. 107 (2007) 4111–4132.
[2] T. Matsunaga, F. Buchter, P. Mauron, A. Bielman, Y. Nakamori, S. Orimo, Hydrogen storage properties of $Mg(BH_4)_2$, J. Alloys Compd. 459 (2008) 583–588.
[3] G.L. Soloveichik, Y. Gao, J. Rijssenbeek, M. Andrus, S. Kniajanski, R.C. Bowman, S.-J. Hwang, J.C. Zhao, Magnesium borohydride as a hydrogen storage material:

properties and dehydrogenation pathway of unsolvated $Mg(BH_4)_2$, Int. J. Hydrog. Energy 34 (2009) 916–928.
[4] M. Paskevicius, L. Jepsen, P. Schouwink, R. Černý, D.B. Ravnsbæk, Y. Filinchuk, M. Dornheim, F. Besenbacher, T.R. Jensen, Metal borohydrides and derivatives – synthesis, structure and properties, Chem. Soc. Rev. 46 (2017) 1565–1634.
[5] E. Hadjixenophontos, E.M. Dematteis, N. Berti, A.R. Wołczyk, P. Huen, M. Brighi, T.T. Le, A. Santoru, S.P. GharibDoust, F. Peru, A.H. Dao, Y. Liu, M. Heere, A review of the MSCA ITN ECOSTORE—novel complex metal hydrides for efficient and compact storage of renewable energy as hydrogen and electricity, Inorganics 8 (2020) 17.
[6] Y. Nakamori, K. Miwa, A. Ninomiya, H. Li, N. Ohba, S. Towata, A. Züttel, S. Orimo, Correlation between thermodynamical stabilities of metal borohydrides and cation electronegativities: first-principles calculations and experiments, Phys. Rev. B 74 (2006), 045126.
[7] F. Maximilian, Z.-K. Zhirong, H. Jianjiang, R. Arne, W. Peter, The kinetic properties of $mg(BH_4)_2$ infiltrated in activated carbon, Nanotechnology 20 (2009), 204029.
[8] H.W. Li, K. Kikuchi, Y. Nakamori, K. Miwa, S. Towata, S. Orimo, Effects of ball milling and additives on dehydriding behaviors of well-crystallized $Mg(BH_4)_2$, Scr. Mater. 57 (2007) 679–682.
[9] R.J. Newhouse, V. Stavila, S.-J. Hwang, L.E. Klebanoff, J.Z. Zhang, Reversibility and improved hydrogen release of magnesium borohydride, J. Phys. Chem. C 114 (2010) 5224–5232.
[10] M. Heere, O. Zavorotynska, S. Deledda, M.H. Sorby, D. Book, T. Steriotis, B. C. Hauback, Effect of additives, ball milling and isotopic exchange in porous magnesium borohydride, RSC Adv. 8 (2018) 27645–27653.
[11] V.I. Bakhmutov, Dihydrogen Bonds: Principles, Experiments, and Applications, John Wiley & Sons, Hoboken, New Jersey, 2008.
[12] O.A. Filippov, N.V. Belkova, L.M. Epstein, E.S. Shubina, Chemistry of boron hydrides orchestrated by dihydrogen bonds, J. Organomet. Chem. 747 (2013) 30–42.
[13] G. Soloveichik, J.-H. Her, P.W. Stephens, Y. Gao, J. Rijssenbeek, M. Andrus, Ammine magnesium borohydride complex as a new material for hydrogen storage: structure and properties of $mg(BH_4)_2{\cdot}2NH_3$, Inorg. Chem. 47 (2008) 4290–4298.
[14] Y. Yang, Y. Liu, Y. Li, M. Gao, H. Pan, Heating rate-dependent dehydrogenation in the thermal decomposition process of $mg(BH_4)_2{\cdot}6NH_3$, J. Phys. Chem. C 117 (2013) 16326–16335.
[15] T. He, H. Wu, J. Chen, W. Zhou, G. Wu, Z. Xioong, Alkali and alkaline-earth metal borohydride hydrazinates: synthesis, structures and dehydrogenation, Phys. Chem. Chem. Phys. 15 (2013) 10478–10493.
[16] J. Chen, Y.S. Chua, H. Wu, Z. Xiong, T. He, W. Zhou, X. Ju, M. Yang, G. Wu, P. Chen, Synthesis, structures and dehydrogenation of magnesium borohydride – ethylenediamine composites, Int. J. Hydrog. Energy 40 (2015) 412–419.
[17] M. Matsuo, Y. Nakamori, S. Orimo, H. Maekawa, H. Takamura, Lithium superionic conduction in lithium borohydride accompanied by structural transition, Appl. Phys. Lett. 91 (2007), 224103.
[18] H. Maekawa, M. Matsuo, H. Takamura, M. Ando, Y. Noda, T. Karahashi, S. Orimo, Halide-stabilized $LiBH_4$, a room-temperature lithium fast-ion conductor, J. Am. Chem. Soc. 131 (2009) 894–895.
[19] M. Matsuo, A. Remhof, P. Martelli, R. Caputo, M. Ernst, Y. Miura, T. Sato, H. Oguchi, H. Maekawa, H. Takamura, A. Borgschulte, A. Züttel, S. Orimo, Complex hydrides with $(BH_4)^-$ and $(NH_2)^-$ anions as new lithium fast-ion conductors, J. Am. Chem. Soc. 131 (2009) 16389–16391.
[20] M.B. Ley, S. Boulineau, R. Janot, Y. Filinchuk, T.R. Jensen, New Li-ion conductors and solid state hydrogen storage materials: $LiM(BH_4)_3Cl$, M = La, Gd. J. Phys. Chem. C 116 (2012) 21267–21276.
[21] T.J. Udovic, M. Matsuo, A. Unemoto, N. Verdal, V. Stavila, A.V. Skripov, J.J. Rush, H. Takamura, S. Orimo, Sodium superionic conduction in $Na_2B_{12}H_{12}$, Chem. Commun. 50 (2014) 3750–3752.
[22] W.S. Tang, M. Matsuo, H. Wu, V. Stavila, W. Zhou, A.A. Talin, A.V. Soloninin, R. V. Skoryunov, O.A. Babanova, A.V. Skripov, A. Unemoto, S. Orimo, T.J. Udovic, Liquid-like ionic conduction in solid lithium and sodium monocarba-*closo*-decaborates near or at room temperature, Adv. Energy Mater. 6 (2016) 1502237.
[23] M. Brighi, P. Schouwink, Y. Sadikin, R. Černý, Fast ion conduction in garnet-type metal borohydrides $Li_3K_3Ce_2(BH_4)_{12}$ and $Li_3K_3La_2(BH_4)_{12}$, J. Alloys Compd. 662 (2016) 388–395.
[24] K. Yoshida, T. Sato, A. Unemoto, M. Matsuo, T. Ikeshoji, T.J. Udovic, S. Orimo, Fast sodium ionic conduction in $Na_2B_{10}H_{10}$-$Na_2B_{12}H_{12}$ complex hydride and application to a bulk-type all-solid-state battery, Appl. Phys. Lett. 110 (2017), 103901.
[25] J. Lefevr, L. Cervini, J.M. Griffin, D. Blanchard, Lithium conductivity and ion dynamics in $LiBH_4/SiO_2$ solid electrolytes studied by solid-state NMR and quasi-elastic neutron scattering and applied in lithium-sulfur batteries, J. Phys. Chem. C 122 (2018) 15264–15275.
[26] S. Kim, H. Oguchi, N. Toyama, T. Sato, S. Takagi, T. Otomo, D. Arunkumar, N. Kuwata, J. Kawamura, S. Orimo, A complex hydride lithium superionic conductor for high-energy-density all-solid-state lithium metal batteries, Nat. Commun. 10 (2019) 1081.
[27] L. Duchêne, A. Remhof, H. Hagemann, C. Battaglia, Status and prospects of hydroborate electrolytes for all-solid-state batteries, Energy Storage Mater. 25 (2020) 782–794.
[28] F. Murgia, M. Brighi, R. Černý, Room-temperature-operating Na-ion solid state battery with complex hydride as electrolyte, Electrochem. Commun. 106 (2019), 106534.
[29] https://www.usgs.gov/centers/national-minerals-information-center/magnesium-statistics-and-information.
[30] R. Mohtadi, M. Matsui, T.S. Arthur, S.-J. Hwang, Magnesium borohydride: from hydrogen storage to magnesium battery, Angew. Chem. Int. Ed. 51 (2012) 9780–9783.
[31] T. Ikeshoji, E. Tsuchida, S. Takagi, M. Matsuo, S. Orimo, Magnesium ion dynamics in $mg(BH_4)_{2(1-x)}X_{2x}$ (x = cl or $AlH_4$) from first-principles molecular dynamics simulations, RSC Adv. 4 (2014) 1366.
[32] S. Higashi, K. Miwa, M. Aoki, K. Takechi, A novel inorganic solid state ionic conductor for rechargeable mg batteries, Chem. Commun. 50 (2014) 1320–1322.
[33] E. Roedern, R.S. Kühnel, A. Remhof, C. Battaglia, Magnesium ethylenediamine borohydride as solid-state electrolyte for magnesium batteries, Sci. Rep. 7 (2017) 46189.
[34] I.E. Golub, M. Heere, V. Gounaris, X. Li, T. Steenhaut, J. Wang, K. Robeyns, H.-W. Li, I. Dovgaliuk, K. Ikeda, G. Hautier, Y. Filinchuk, Structural insight into the magnesium borohydride – ethylenediamine solid-state Mg-ion electrolyte system, Dalton Trans. 52 (2023) 2404–2411.
[35] T. Tsang, T.C. Farrar, Nuclear magnetic relaxation studies of internal rotations and phase transitions in borohydrides of lithium, sodium, and potassium, J. Chem. Phys. 50 (1969) 3498–3502.
[36] A.V. Skripov, A.V. Soloninin, O.A. Babanova, Nuclear magnetic resonance studies of atomic motion in borohydrides, J. Alloys Compd. 509S (2011) S535–S539.
[37] A.V. Soloninin, O.A. Babanova, A.V. Skripov, H. Hagemann, B. Richter, T. R. Jensen, Y. Filinchuk, NMR study of reorientational motion in alkaline-earth borohydrides: β and γ phases of $Mg(BH_4)_2$ and α and β phases of $Ca(BH_4)_2$, J. Phys. Chem. C 116 (2012) 4913–4920.
[38] A.V. Skripov, M. Dimitrievska, O.A. Babanova, R.V. Skoryunov, A.V. Soloninin, F. Morelle, Y. Filinchuk, A. Faraone, H. Wu, W. Zhou, T.J. Udovic, Low-temperature rotational tunneling of tetrahydroborate anions in lithium benzimidazolate-borohydride $Li_2(bIm)BH_4$, J. Phys. Chem. C 123 (2019) 20789–20799.
[39] A.V. Skripov, A.V. Soloninin, M.B. Ley, T.R. Jensen, Y. Filinchuk, Nuclear magnetic resonance study of $BH_4$ reorientations and Li diffusion in $LiLa(BH_4)_3Cl$, J. Phys. Chem. C 117 (2013) 14965–14972.
[40] A.V. Skripov, A.V. Soloninin, O.A. Babanova, R.V. Skoryunov, Nuclear magnetic resonance studies of atomic motion in borohydride-based materials: fast anion reorientations and cation diffusion, J. Alloys Compd. 645 (2015) S428–S433.
[41] K. Kweon, J.B. Varley, P. Shea, N. Adelstein, P. Mehta, T.W. Heo, T.J. Udovic, V. Stavila, B.C. Wood, Structural, chemical, and dynamical frustration: origins of superionic conductivity in *closo*-borate solid electrolytes, Chem. Mater. 29 (2017) 9142–9153.
[42] A.V. Skripov, A.V. Soloninin, O.A. Babanova, R.V. Skoryunov, Anion and cation dynamics in polyhydroborate salts: NMR studies, Molecules 25 (2020) 2940.
[43] M. Heere, A.-L. Hansen, S. Payandeh, N. Aslan, G. Gizer, M.H. Sørby, B.C. Hauback, C. Pistidda, M. Dornheim, W. Lohstroh, Dynamics of porous and amorphous magnesium borohydride to understand solid state mg-ion-conductors, Sci. Rep. 10 (2020) 9080.
[44] P.C. Tsai, S. Mair, J. Smith, D.M. Halat, P.H. Chien, K. Kim, D. Zhang, Y. Li, L. Yin, J. Liu, S.H. Lapidus, J.A. Reimer, N.P. Balsara, D.J. Siegel, Y.M. Chiang, Double paddle-wheel enhanced sodium ion conduction in an antiperovskite solid electrolyte, Adv. Energy Mater. (2022) 2203284.
[45] Y. Filinchuk, B. Richter, T.R. Jensen, V. Dmitriev, D. Chernyshov, H. Hagemann, Porous and dense magnesium borohydride frameworks: synthesis, stability, and reversible absorption of guest species, Angew. Chem. Int. Ed. 50 (2011) 11162–11166.
[46] J. Huot, F. Cuevas, S. Deledda, K. Edalati, Y. Filinchuk, T. Grosdidier, B. C. Hauback, M. Heere, T.R. Jensen, M. Latroche, S. Sartori, Mechanochemistry of metal hydrides: recent advances, Materials 12 (2019) 2778.
[47] A. Abragam, The Principles of Nuclear Magnetism, Clarendon Press, Oxford, 1961.
[48] A.V. Skripov, A.V. Soloninin, O.A. Babanova, H. Hagemann, Y. Filinchuk, Nuclear magnetic resonance study of reorientational motion in α-$Mg(BH_4)_2$, J. Phys. Chem. C 114 (2010) 12370–12374.
[49] D.T. Shane, L.H. Rayhel, Z. Huang, J.-C. Zhao, X. Tang, V. Stavila, M.S. Conradi, Comprehensive NMR study of magnesium borohydride, J. Phys. Chem. C 115 (2011) 3172–3177.
[50] M. Eagles, B. Sun, B. Richter, T.R. Jensen, Y. Filinchuk, M.S. Conradi, NMR investigation of nanoporous γ-$mg(BH_4)_2$ and its thermally induced phase changes, J. Phys. Chem. C 116 (2012) 13033–13037.
[51] V. Ban, A.V. Soloninin, A.V. Skripov, J. Hadermann, A. Abakumov, Y. Filinchuk, Pressure-collapsed amorphous $Mg(BH_4)_2$: an ultradense complex hydride showing a reversible transition to the porous framework, J. Phys. Chem. C 118 (2014) 23402–23408.
[52] M. Prager, A. Heidemann, Rotational tunneling and neutron spectroscopy: a compilation, Chem. Rev. 97 (1997) 2933–2966.
[53] J.T. Markert, E.J. Cotts, R.M. Cotts, Hydrogen diffusion in the metallic glass *a*-$Zr_3RhH_{3.5}$, Phys. Rev. B 37 (1988) 6446–6452.
[54] A.V. Skripov, A.V. Soloninin, Y. Filinchuk, D. Chernyshov, Nuclear magnetic resonance study of the rotational motion and the phase transition in $LiBH_4$, J. Phys. Chem. C 112 (2008) 18701–18705.
[55] K. Jimura, S. Hayashi, Reorientational motion of $BH_4$ ions in alkali borohydrides $MBH_4$ (M = Li, Na, K) as studied by solid-state NMR, J. Phys. Chem. C 116 (2012) 4883–4891.
[56] I.J. Lowe, S. Gade, Density-matrix derivation of the spin-diffusion equation, Phys. Rev. 156 (1967) 817–825.